Proceedings of the ASME 2015 Power and Energy Conversion Conference
PowerEnergy2015
June 28-July 2, 2015, San Diego, California
PowerEnergy2015-49472

DESIGN AND CHARACTERIZATION OF A 7.2 KW SOLAR SIMULATOR

Antoine Boubault, Julius Yellowhair, Clifford K. Ho
Sandia National Laboratories
P.O. Box 5800, MS-1127
Albuquerque, NM 87185-1127, USA
anbouba@sandia.gov

ABSTRACT

A 7.2 kW radiative solar simulator was designed in order to perform accelerated testing on absorber materials for concentrating solar power (CSP) technologies. Computer-aided design (CAD) software integrating a ray-tracing tool was used to select appropriate components and optimize their positioning in order to achieve the desired concentration. The simulator comprises four identical units, each made out of an ellipsoidal reflector, a metal halide lamp and an adjustable holding system. A single unit was characterized and shows an experimental average irradiance of 257 kW m^{-2} on a 25.4 mm (1 inch) diameter spot. Shape, spot size and average irradiance are in good agreement with the model predictions. The innovative four-lamp solar simulator potentially demonstrates peak irradiance of 1140 kW m^{-2} and average irradiance of 878 kW m^{-2} over a 25.4 mm diameter spot. The costs per radiative and electric watt are calculated at \$2.31 W^{-1} and \$1.99 W^{-1}, respectively.

INTRODUCTION

In concentrating solar power applications, high temperatures (> 700°C) are required to achieve high power-cycle efficiencies. Novel materials are being developed to absorb highly concentrated solar radiation (≥ 1000 kW m^{-2}) while maintaining low heat losses. One way to achieve this goal is to use selective coatings that have a high solar absorptance and low thermal emittance. The extreme conditions in which these materials generally operate trigger specific aging mechanisms which alter their performance over time. Accelerated testing is required to test their durability in an acceptable timescale (a few hours to a few months).

Testing under high solar fluxes may be considered using conventional outdoor solar furnaces. This approach usually benefits from realistic solar radiation conditions. However, accelerated testing under well-controlled environments in solar furnace is a challenge because of weather fluctuations and operation during daylight hours only. In order to overcome these limitations and provide a low-cost solution for testing durability of absorber materials, a solar simulator is designed and built.

Several high-flux solar simulators exist that are capable of reaching very high fluxes (>10000 kW m^{-2}). The Paul Scherrer Institute (PSI) [1,2], the Eidgenössische Technische Hochschule (ETH) [3] and the Federal Institute of Technology in Lausanne (EPFL) [4] in Switzerland, the German Aerospace Center (DLR), the University of Minnesota [5], the Texas A&M University at Qatar [6], the Australian National University and the Ecole Polytechnique Fédérale de Lausanne (EPFL) have designed and built such systems for studying thermochemical processes and materials under very high concentration. But such systems are typically associated with significant costs (>\$100k), difficult assembly and operation due to their large size, customized components, and significant safety requirements. Massachusetts Institute of Technology (MIT) built a low cost (> \$10k), reduced-size solar simulator [7], but their peak irradiance was lower than 100 kW m^{-2} due to poor concentrating reflectors. In this paper, we investigate the possibility of building an effective low-cost solar simulator using commercial-off-the-shelf (COTS) components, which can be operated continuously.

A ray-tracing model coupled with an optimization routine that maximizes the concentration is developed with consideration of the focal length and aim points of each reflector. The solar simulator is made out of four 1800 W high-intensity metal halide arc lamps with electro-formed nickel-

based silver-coated elliptical reflectors. It is low-cost (< $15k), compact (< 10 m^3), flexible (movable, adjustable flux distribution and power), and is able to operate around-the-clock for extended-time testing. Its vertical design simplifies positioning of the lamps and the target and mitigates the typical safety issues of a horizontal design (direct exposure). The model is validated by experimental characterization of a one-lamp system.

SOLAR SIMULATOR DESIGN AND COMPONENTS

One goal of using a solar simulator is to duplicate the solar spectrum and beam characteristics with high-powered lamps and reflectors that can be used indoors. The simulator can then be used as a substitute for solar furnaces when outdoor weather conditions are unfavorable or at night to increase the available testing time.

The concentration is achieved by a source of light coupled with a concentrating element. The design that is most commonly used is the combination of a lamp which emits near-solar light with an ellipsoidal reflector. The lamp source is placed at the primary focus F_1 of the ellipsoid so the light is concentrated at the secondary focus F_2 (see Figure 1). A real source of light is a filament or arc—not a point source—causing the rays to be reflected away from F_2 (for example points A, B and C on Figure 1). In the case of an extended source, the highest concentration factor may not be obtained at the secondary focus point, depending on the arc dimensions and position with respect to the primary focus.

The simulation of different configurations with off-the-shelf reflectors and lamps allows us to select the components that achieve high concentration ratio at a relatively low total cost (< $15k). Several reflectors are considered. Optiforms E813-7 [8] ellipsoidal reflectors combine large acceptance angle (~94.6°) and large rim angle (31.3°), high concentration factor and interfocal length of 812.8 mm which complies with the volume constraint of the facility (10 m^3). The reflector is made out of nickel coated with silver to enhance the reflectance, and a transparent silicon dioxide thin layer to protect against oxidation/corrosion. The spectral hemispherical reflectivity of silver is plotted in Figure 2.

Different lamps are considered according to different parameters such as power, arc length, spectral distribution and cost. The smaller the lamp arc, the higher the concentration. Among the multiple commercial lamps, two families are commonly used to simulate the solar light: Xenon and the metal halides lamps. Figure 3 shows the spectral power distribution of a typical Xenon lamp and a 2500 HMI metal halide lamp compared with the solar spectral distribution. We observe that both lamps do not match perfectly the solar spectrum, both Xenon and metal halides have narrow energy peaks that could generate unrealistic effects during tests. However, the metal halide tends to adopt a closer shape than the Xenon (discussed more in details by Kockott [9]). They have also twice as high luminous efficacy and are available at cheaper compared to similar power Xenon lamps.

Single-ended lamps are selected to avoid fixtures in front of the reflector which would partially intercept the concentrated light. The HMI 1800 W/SE XS metal halide lamp, shown in Figure 4, has a high luminous efficacy (92 lm W^{-1}), short arc length (12.7 mm), acceptable service life of 750 hours, and can be run in any position [10]. Figure 5 shows an assembled lamp-reflector unit.

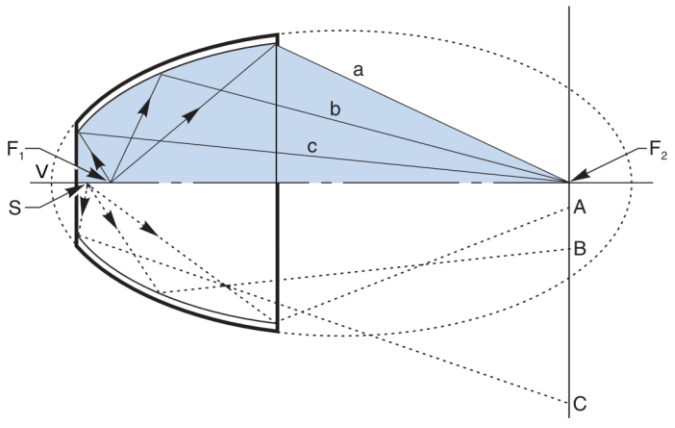

Figure 1. Ray optical paths for different source locations. Points A, B and C are images of point sources S located close to the primary focus F_1. Point V is defined as the vertex of the reflector. The distance between F_1 and F_2 is the interfocal length.

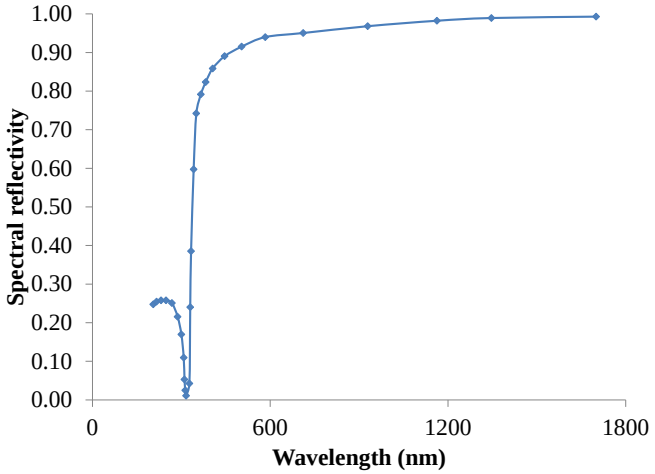

Figure 2. Spectral hemispherical reflectivity of silver

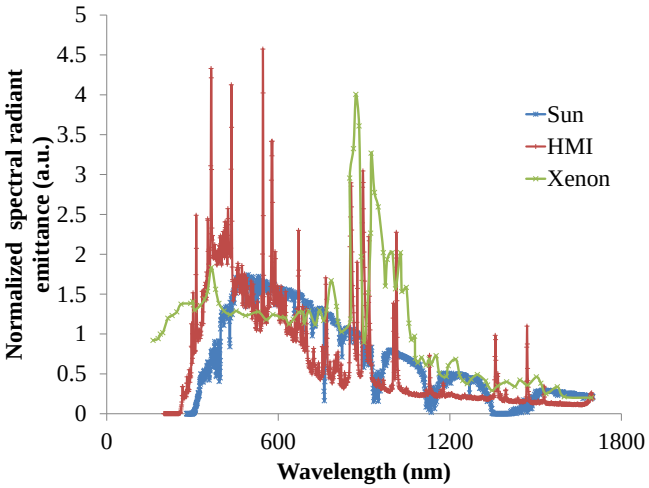

Figure 3. Spectral intensity of typical Xenon [11] and metal halide arcs (OSRAM data for HMI 2500 W/SE XS) compared to the solar spectrum [12]. The data are normalized to have an average value equal to 1.

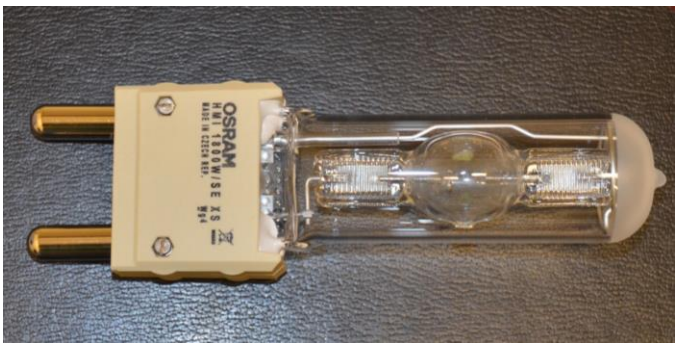

Figure 4. HMI 1800 W/SE XS metal halide lamp. Total length: ~ 200 mm.

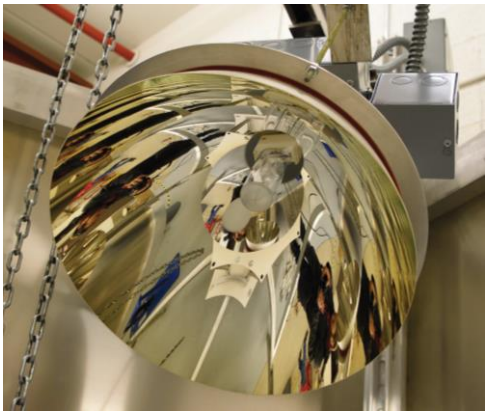

Figure 5. Optiforms E813-7 reflector with HMI 1800 W/SE XS lamp

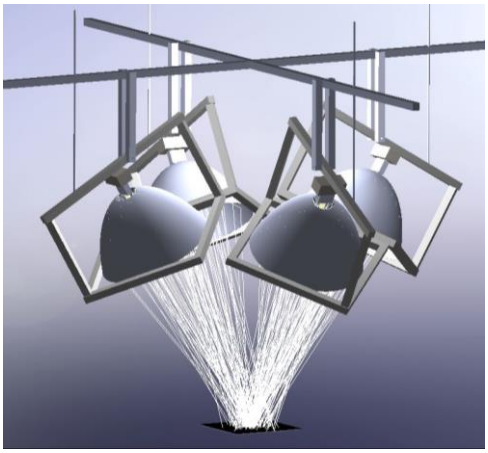

Figure 6. Four-lamp solar simulator design

To achieve an average irradiance of 1000 kW m^{-2} over a 25.4 mm (1 inch) diameter surface, two main options are considered: (1) use of a single reflector with a high power lamp or (2) use of multiple lamp-reflector units at a lower power. Option 2 is elected in order to limit the risk of overheating and damage to the reflector as it was previously observed in the literature [13]. In addition, multiple units allow better control of the irradiance and flux profile as well as higher durability and cheaper maintenance (lamp replacement). The significant cost of the ballasts and ignitors—electric components that enable striking of the metal halide lamps— is also considered to choose the best combination between power and number of lamps. The final design consists of four lamp-reflector units with 1800 W lamps. Their luminous flux of 165000 lumens yields calculated electric-to-radiative efficiency of 86%, corresponding to an emitted radiative power of 1550 W per lamp (6200 W total). The lamps do not require forced convection cooling which reduces materials, design and safety costs. A four-channel ballast was found to allow individual power supply to each of the four 1800 W lamps. This is a much cheaper alternative compared to cost of four separated ballasts. The specular total reflectance of the reflectors is calculated over the metal halide lamp spectrum (shown in Figure 3) and is 0.875.

We opt for a vertical beam-down design so that test samples can be held horizontally while the effect of gravity on the positioning system is minimized. This solution also mitigates the safety hazards by reducing the risk of direct exposure to the lamp beams. Figure 6 shows the final design of the solar simulator, drawn in SolidWorks.

The costs for the four-lamp simulator are provided in Table 1. Only the components needed to assemble the solar simulator are shown i.e. labor to assemble the system is not included. Additional auxiliary components, such as test bed, data acquisition system and instrumentation can be added based on the user's needs.

Table 1. Bill of materials for the four-lamp solar simulator

Component(s)	Manufacturer	Cost ($)
1800 W metal halide lamps with socket mounts (x 4)	Osram	1,500
Elliptical reflectors with 813 mm inter-focal distance (x 4)	Optiforms, Inc.	5,250
Ballast with 4 ignitors	Power Gems Ltd.	6,000
Sample stage/holder	Custom built at SNL	100
Structure (76.2 mm box beams and angle iron)	Custom built at SNL	500
Enclosure	Custom built at SNL	500
Electrical enclosure boxes (to enclose ignitor and lamp socket) & wiring	COTS	50
Mounting hardware for the reflector and lamps	COTS and custom	400
Total		14,300

NUMERICAL ANALYSIS

Solidworks add-in APEX enables ray-tracing analyses via a Monte-Carlo method. Modelization of the solar simulator is used to optimize the relative positions between the lamp, the reflector and the target, as well as to simulate the irradiance maps at the secondary focus.

The arc is not precisely defined as it is an emitting volume instead of a filament. Previous studies [4,5] chose to model the arc by a 2 mm diameter cylinder of the specified arc length. We adopt a similar approach considering a 12.7 mm × 2 mm cylinder where rays are emitted by the external surface equally in every direction of the hemisphere. Studies were done [14] and are underway to propose more realistic models for such arc sources. A parametric study is performed considering the average irradiance on a 25.4 mm (1 inch) diameter disk corresponding to the size of the samples that are to be tested. A single lamp-reflector unit is studied. The reflector axis is aligned with the center of the 127 mm × 127 mm (5 inch × 5 inch) target (see Figure 7).The target is meshed with 0.254 mm × 0.254 mm cells. The arc is centered on the primary focus of the reflector ($F_1S = 0$) and the target surface is positioned on the secondary focus ($F_1T = 812.8$ mm). This is the "nominal" configuration. All simulations are run with 250,000 emitted rays per lamp.

Starting from this nominal configuration, the positions of both the lamp and the target are varied and optimized along the reflector axis to achieve the maximum peak irradiance in the center of the target. The optimization process uses an iterative Nelder-Mead method. A ray-tracing simulation is performed each iteration and the position of the lamp and target are modified simultaneously.

The routine converges for a lamp position that is 1 mm ($F_1S = 1.0$ mm) lower than the initial position, and for a target position 19.2 mm closer to the reflector ($F_1T = 793.6$ mm). The average irradiance on the 25.4 mm diameter disk is 568 kW m^{-2} (288 W). This is a 1.8% increase compared to the nominal configuration.

Figure 8 shows the flux distribution in the nominal configuration. The average irradiance on a centered 25.4 mm diameter disk is 558 kW m^{-2}. The total flux on the disk is 283 W which is equivalent to 18.3% of the emitted flux (1550 W) and 15.7% of the electric power (1800 W). The peak irradiance is 1130 kW m^{-2}.

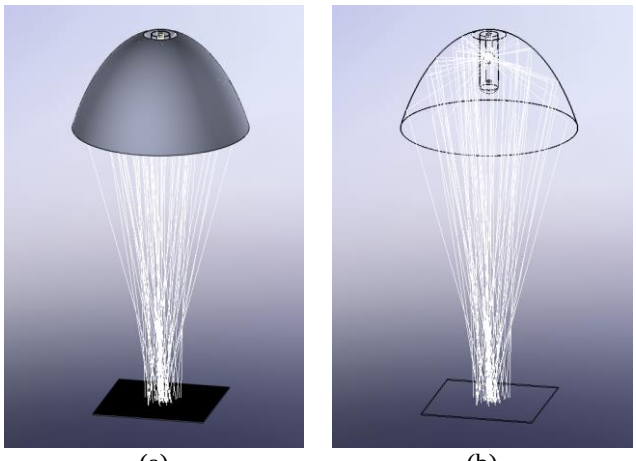

Figure 7. Lamp/reflector assembly in front of a sample. (a) opaque view and (b) wireframe view.

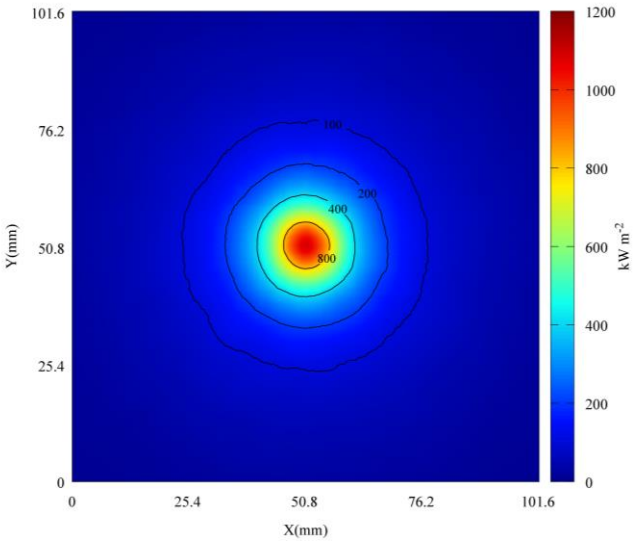

Figure 8. Incident flux distribution for one lamp-reflector unit in the nominal configuration ($F_1S = 0$, $F_1T = 812.8$ mm)

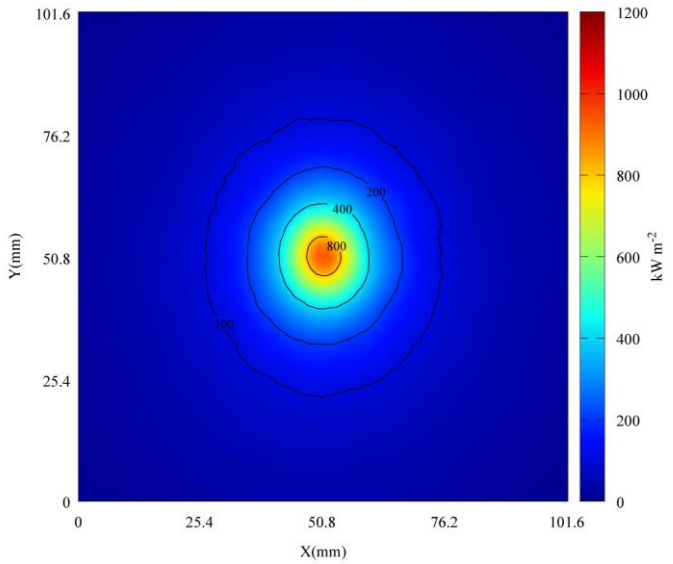

Figure 9. Incident flux distribution for one lamp-reflector unit tilted at 31.0° (located at top of flux map), in the nominal configuration ($F_1S = 0$, $F_1T = 812.8$ mm)

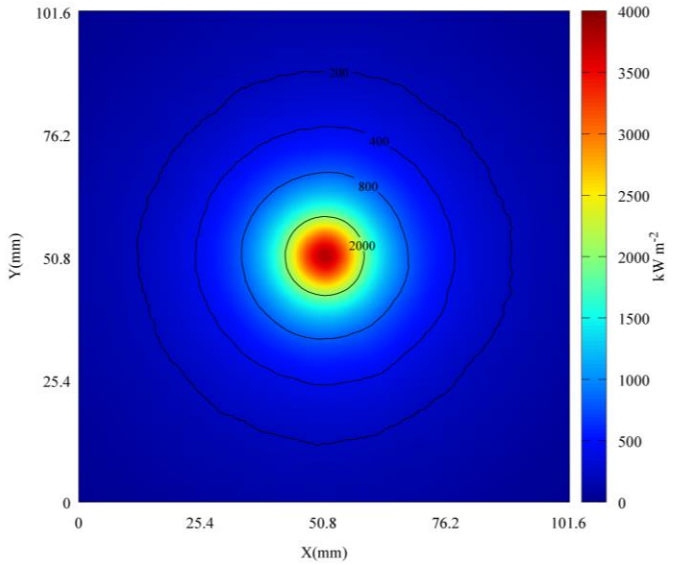

Figure 10 Incident flux distribution for four lamp-reflector units in the nominal configuration ($F_1S = 0$, $F_1T = 812.8$ mm)

In the four-lamp design, the lamp-reflector units are all tilted with the same angle relative to the target normal. This affects the flux profile. The tilt angle is determined by the spacing between the reflectors and the distance to the target. The spacing is chosen small so the view factor between the reflectors and the target is maximized, but large enough to provide clearance for rotational movements of the reflectors. Given the dimensions of the reflectors and their rotational movements, we set a spacing of 450 mm between their vertices.

In the nominal configuration (lamp arc centered on primary focus and target on secondary focus), the tilt angle is 31.0°. Figure 9 shows the incident flux map on the target surface resulting from a single tilted lamp-reflector unit. The average irradiance on the 25.4 mm diameter disk is 507 kW m^{-2} which is 9.1% less than in a perpendicular position.

The flux profile resulting from the four lamps in the nominal configuration is simulated and shown in Figure 10. The profile looks similar to that of a not tilted single unit (see Figure 8). The four oval profiles compensate and result in an axisymmetric profile. The average irradiance on the 25.4 mm diameter disk is 2029 kW m^{-2}. Optimization of the arc and target positions with the Nelder-Mead method gives $F_1S = 2.8$ mm and $F_1T = 785.8$ mm, with an optimal tilt angle of 32.1°. The average irradiance over the disk is in this case 2091 kW m^{-2} which is a 3.1% increase compared to the nominal configuration. The total flux on the target is 3811 W which is 61.5% of the total emitted flux and 52.9% of the electric power. The peak irradiance is 3998 kW m^{-2}.

CHARACTERIZATION METHOD

A single lamp-reflector system is mounted to characterize the flux profile of one unit. The lamp is centered on the primary focus of the reflector as in the nominal configuration. In the experimental characterization, the lamp position is not changed. Only the position and inclination of the target are varied.

The system is set up in an enclosed structure that is 1270 mm × 1270 mm × 2130 mm (3.435 m^3). The walls are made of polycarbonate which filters UV radiation. A height-adjustable table enables positioning the target plane closer or further from the reflector.

The target irradiance is measured with a Kendall radiometer (Medtherm Corp.) calibrated by Technical Measurements, Inc. The radiometer is water-cooled and measures up to 1500 kW m^{-2} (1500 suns) on a 2 mm diameter sensitive area. A stand is designed and built for holding the radiometer and future samples. Figure 11 is a picture of the one-lamp simulator with the Kendall radiometer used to calibrate the flux maps.

A white board is used to map the irradiance at the reflector focus with a camera equipped with neutral density filters. It is made of RSLE-57(Zircar Refractory Composites, Inc.), a low-expansion, high-strength reinforced silica matrix composite. It is typically used as an insulator in high temperature applications up to 1200°C. Its surface texture provides a near-Lambertian surface which is ideal to perform flux mapping.

Flux maps are obtained for normal and a 30° incidence on the target. The camera is positioned in a near-normal incidence relative to the target. Typical camera settings used are: manual mode, 55 mm focal length, 1/200 second shutter speed, f/36 aperture, no flash, and RAW image format.

Figure 11. Kendall radiometer mounted on a holding system for irradiance calibration measurement

Figure 12. Flux mapping with a camera and a white board at 30° tilt angle

In order to predict the flux map that would be obtained in the four-lamp design (not yet mounted), the map obtained for a single tilted lamp is rotated by 90° angles and summed up to represent flux from the other three lamp-reflector systems (see illustration Figure 6). Identical performance from each of the lamp-reflector system is assumed.

The flux maps and the average irradiance on the 25.4 mm diameter spot obtained are compared with the ray-tracing simulations.

RESULTS AND DISCUSION

The lamp is progressively set at its maximum power via the ballast dimming function. Flickering is observed while the lamp heats up. Measurements are performed at least 30 minutes after the lamp is lit to ensure steady state is reached.

The target position is manually adjusted at the maximum experimental average irradiance position. Figure 13 shows the peak and the average irradiance measured for several positions of the target, above and below the nominal interfocal distance of 812.8 mm. We observe that the experimental peak irradiance is higher at a shorter distance from the reflector and reaches a maximum of 340 kW m^{-2} at about 13 mm above the secondary focus. This is in good agreement with the model which predicts a maximum average irradiance about 14 mm above the secondary focus (558 kW m^{-2}) when the arc is centered on the primary focus. Sensitivity of the irradiance to the focus-to-target distance is low (variations < 50 kW m^{-2} over 10 cm), as predicted by the model. The experimentally optimized distance is F_1T = 800 mm which is slightly different from that of the predicted maximum average irradiance (~F_1T = 787 mm).

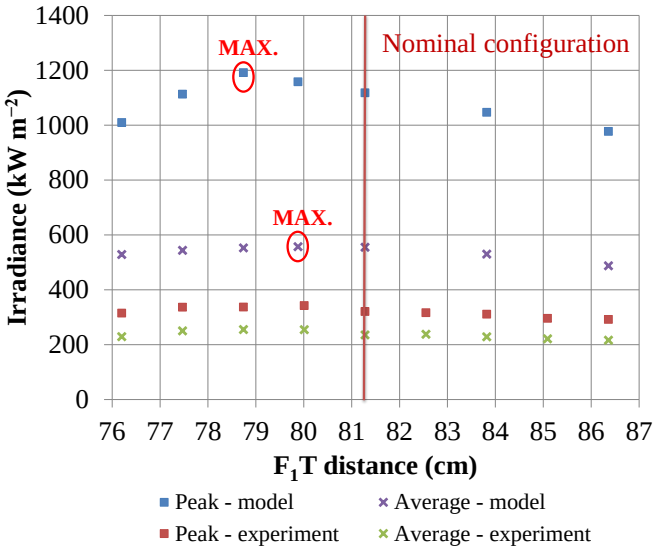

Figure 13. Simulated and experimental peak and average irradiance over a 25.4 mm (1 inch) diameter spot for several focus-to-target distances. The nominal configuration is represented by the red line.

Figure 14 shows the measured flux map in this configuration. About 90% of the total incident energy is contained in about 122 mm diameter of the spot centered on its peak value. The average irradiance on a 25.4 mm diameter spot centered on the peak is 255 kW m^{-2}. This is 2.2 times lower (45.7%) than the predicted average irradiance in the nominal configuration (558 kW m^{-2}). We attribute this difference to two possible reasons: (1) in the model, reflector geometry is assumed "perfect" and no optical error is considered; and (2) the arc cylinder geometry might not be representative of the real arc source.

The influence of the arc size is investigated by varying the diameter of the cylindrical element from 2 mm to 7 mm. The different irradiance profiles obtained are shown in Figure 15. There is good agreement between the experimental and predicted "shape" of the flux profile, even though the model predicts much higher peak irradiance for an arc diameter of 2 mm (3.3 times higher). The geometry and dimensions of the arc source highly impact the concentration ratio and the irradiance profile at the focus as noted by Alxneit et al. [13]. Increasing the arc diameter reduces the peak irradiance and flattens the profile. We choose to set the arc diameter to a value of 6 mm to better represent the experimental results. Future development will include characterization of the intensity profile of the lamp arc to improve the arc model.

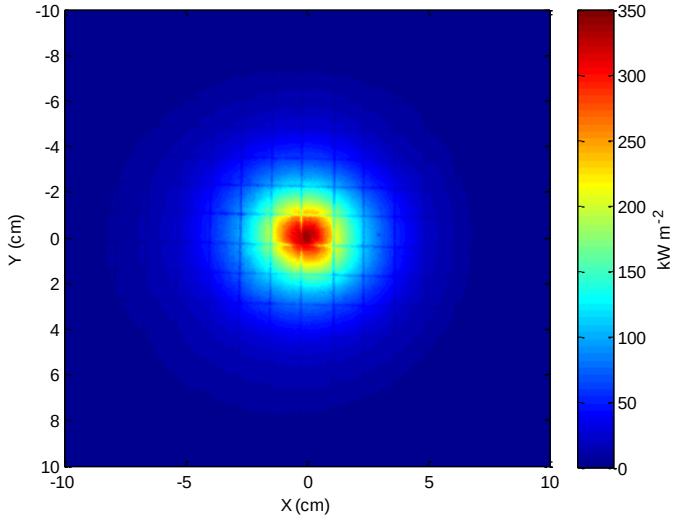

Figure 14. Incident flux distribution at normal incidence ($F_1S = 0$, $F_1T = 800$ mm) and normal incidence. The grid seen in the image has size equal to 0.5 in × 0.5 in (12.7 mm × 12.7 mm).

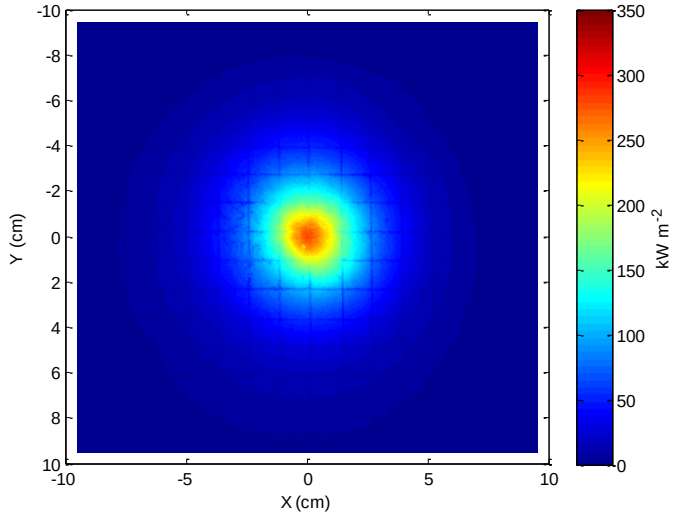

Figure 16. Incident flux distribution with a tilt angle of 30° ($F_1S = 0$, $F_1T = 800$ mm). The grid seen in the image has size equal to 0.5 in × 0.5 in (12.7 mm × 12.7 mm). The lamp unit is located at the top of the flux map.

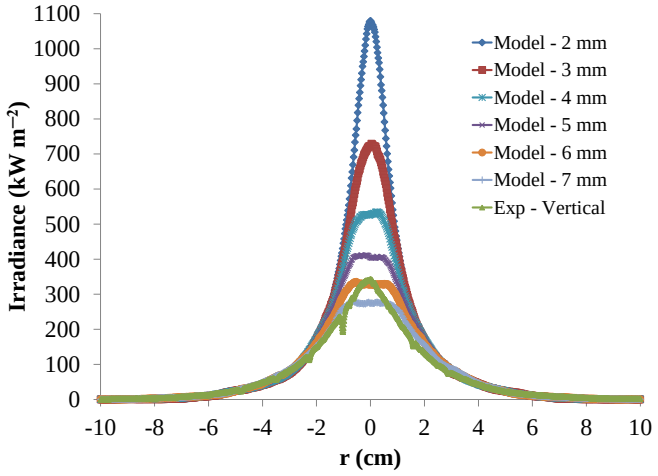

Figure 15. Simulated irradiance profiles depending on the arc diameter compared with the experimental incident flux distribution ($F_1S = 0$, $F_1T = 800$ mm).

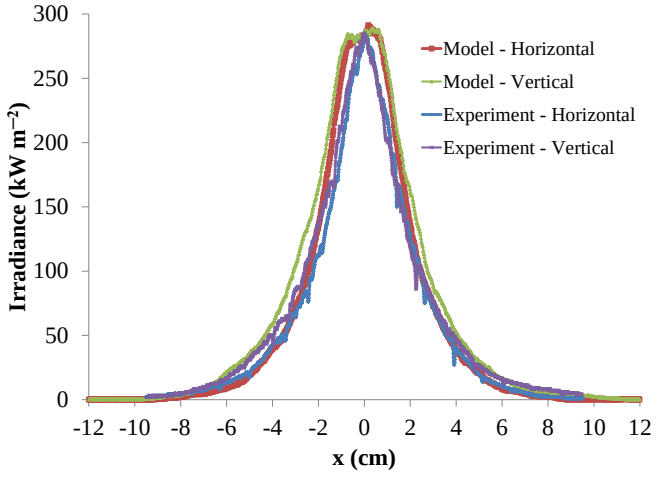

Figure 17. Slice plots of the experimental (experiment) and predicted (model) irradiance for a 30° tilted reflector and arc diameter of 6 mm ($F_1S = 0$, $F_1T = 800$ mm).

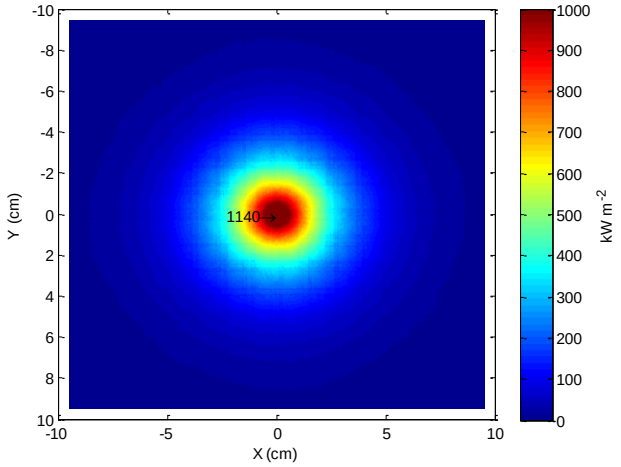

Figure 18. Combined incident flux distribution from experimental results of four identical lamp/reflector units ($F_1S = 0$, $F_1T = 800$ mm). The grid seen in the image has size equal to 0.5 in × 0.5 in (12.7 mm × 12.7 mm).

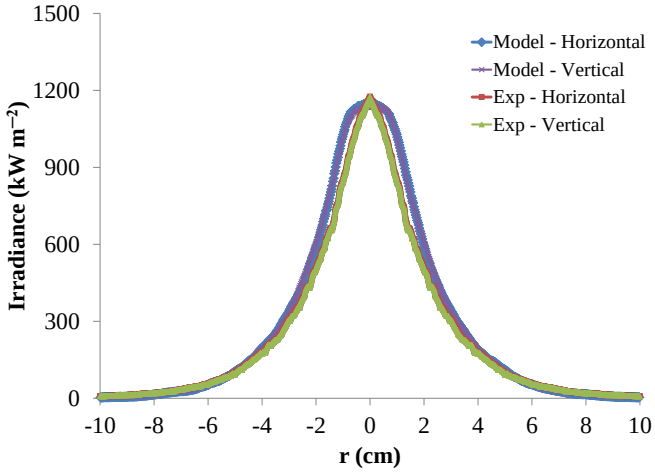

Figure 19. Slice plots of the combined (experiment) and predicted (model) irradiance for four lamp-reflector units with an arc diameter of 6 mm ($F_1S = 0$, $F_1T = 800$ mm).

The effect of the reflector tilt angle is analyzed by tilting the target plane at 30° while keeping the reflector in its original position. Figure 16 and Figure 17 shows the flux map obtained and the corresponding slice plots, respectively.

The tilt angle is responsible for a decrease in the irradiance. The average irradiance over the 25.4 mm diameter spot is 220 kW m^{-2} which is 13.7% less than for a normal incidence. The model predicts a 9.1% decrease. The horizontal and vertical profiles are not significantly "deformed" by the lamp tilting. This behavior is well represented by the model.

The flux map of the four lamp simulator is estimated by rotating Figure 16 four times with an angle of 90°, and then superimposing the four rotated flux map to simulate the beams that would come from the three additional lamps. Since the lamp sources are incoherent, the flux maps can be added directly. The combination is shown in Figure 18 and the slice plots are shown in Figure 19. The combination of the four maps results in an axisymmetric irradiance profile as predicted by the model (see Figure 10). The experimental average irradiance on a 25.4 diameter spot is 878 kW m^{-2}. The experimental peak irradiance is 1140 kW m^{-2}. Finer positioning of the lamp and adjustment of the four lamps could result in higher irradiances.

CONCLUSION

To address the need to perform continuous "on-sun" testing in well-controlled conditions at high-flux and high temperatures, a low-cost solar simulator was designed. The full solar simulator uses four 1800 W (7.2 kW) metal halide lamps and elliptical reflectors. Each lamp-reflector assembly can be positioned independently. The lamps can be dimmed at 50% of their nominal power. The target can be moved closer or further from the lamps to adjust the spot size and the irradiance. This enables flexible control of the flux profile on the test samples.

A model was developed to select the components and optimize the design of the solar simulator. The model results were compared and validated by an experimental setup with a one lamp system and a target that can be tilted. The irradiance maps were combined to estimate the flux map that would be obtained with the four-lamp system. Characterizations showed that optimal positions, spot sizes and profiles are in good agreement with the model, provided the model of the arc source is representative of the real emitter. In current and future development of solar simulators, proper characterization and modelization of the arc source is recommended to ensure accuracy of the simulated flux profiles.

The solar simulator developed potentially demonstrates peak irradiance greater than 1140 kW m^{-2} and average irradiance greater than 878 kW m^{-2} over a 25.4 mm (1 inch) diameter spot. However, the relative position of the arc related to the reflector was not optimal which enables improvements in the achieved irradiance. The costs of the components and materials used to build the simulator were maintained lower than $15k which yields a normalized cost of $2.38 per radiative watt and $1.99 per electric watt. The solar simulator will be used to perform accelerated around-the-clock aging tests. It will also be used for any testing requiring well-controlled and highly-concentrated solar flux.

ACKNOWLEDGMENTS

Sandia National Laboratories is a multi-program laboratory managed and operated by Sandia Corporation, a wholly owned

subsidiary of Lockheed Martin Corporation, for the U.S. Department of Energy's National Nuclear Security Administration under contract DE-AC04-94AL85000. The United States Government and the publisher, by accepting the article for publication, acknowledges that the United States Government retains a non-exclusive, paid-up, irrevocable, world-wide license to publish or reproduce the published form of this manuscript, or allow others to do so, for United States Government purposes.

REFERENCES

[1] Petrasch J, Coray P, Meier A, Brack M, Häberling P, Wuillemin D, et al. A Novel 50kW 11,000 suns High-Flux Solar Simulator Based on an Array of Xenon Arc Lamps. J Sol Energy Eng 2006;129:405–11. doi:10.1115/1.2769701.

[2] Alxneit I, Schmit H. Spectral Characterization of PSI's High-Flux Solar Simulator. J Sol Energy Eng 2011;134:011013–011013. doi:10.1115/1.4005249.

[3] Hirsch D, Zedtwitz P v., Osinga T, Kinamore J, Steinfeld A. A New 75 kW High-Flux Solar Simulator for High-Temperature Thermal and Thermochemical Research. J Sol Energy Eng 2003;125:117–20. doi:10.1115/1.1528922.

[4] Bader R, Haussener S, Lipiński W. Optical Design of Multisource High-Flux Solar Simulators. J Sol Energy Eng 2014;137:021012–021012. doi:10.1115/1.4028702.

[5] Krueger KR, Lipiński W, Davidson JH. Operational Performance of the University of Minnesota 45 kWe High-Flux Solar Simulator. J Sol Energy Eng 2013;135:044501–044501. doi:10.1115/1.4023595.

[6] Sarwar J, Georgakis G, LaChance R, Ozalp N. Description and characterization of an adjustable flux solar simulator for solar thermal, thermochemical and photovoltaic applications. Sol Energy 2014;100:179–94. doi:10.1016/j.solener.2013.12.008.

[7] Codd DS, Carlson A, Rees J, Slocum AH. A low cost high flux solar simulator. Sol Energy 2010;84:2202–12. doi:10.1016/j.solener.2010.08.007.

[8] Optiforms. Optiforms E813-7 Drawing. Optiforms Website 1996. http://www.optiforms.com/drawings/E813-r.pdf (accessed February 11, 2015).

[9] Kockott D, Schoenlein A. To what extent does the radiation of a solar simulator meet a "reference sun"? A quantitative approach. Polym Test 2012;31:710–5. doi:10.1016/j.polymertesting.2012.04.005.

[10] Osram, Sylvania. HMI 1800 W/SE XS Product information. Osram Sylvania Website n.d. https://ecom.sylvania.com/sylvaniab2b/b2b/catalogstart.do?search=advanced (accessed February 12, 2015).

[11] Osram. XBO - theater lamps. Osram Sylvania Website n.d. http://assets.sylvania.com/assets/documents/ENGR_BLTN11.161355cc-1d94-4996-b6cd-a3001fea6f1a.pdf (accessed February 9, 2015).

[12] NREL. Reference Solar Spectral Irradiance: Air Mass 1.5. NREL Website n.d. http://rredc.nrel.gov/solar/spectra/am1.5/ (accessed February 9, 2015).

[13] Alxneit I, Dibowski G. R12.5 Solar Simulator Evaluation Report. 2011.

[14] Wang W, Aichmayer L, Laumert B, Fransson T. Design and Validation of a Low-cost High-flux Solar Simulator using Fresnel Lens Concentrators. Proc SolarPACES 2013 Int Conf 2014;49:2221–30. doi:10.1016/j.egypro.2014.03.235.

